



Contents lists available at ScienceDirect

Catalysis Today

journal homepage: www.elsevier.com/locate/cattod

Alcoxycle: A novel route for glycerol reform into H₂ and CO_x in separate stages

Fabiano Gomes Ferreira de Paula^a, Marcelo Gonçalves Rosmaninho^b,
Ana Paula de Carvalho Teixeira^a, Patterson Patrício de Souza^c, Rochel Montero Lago^{a,*}

^a Universidade Federal de Minas Gerais (UFMG), Av. Antônio Carlos, 6627, Belo Horizonte, 31270-901, Minas Gerais, Brazil

^b Universidade Federal de Ouro Preto (UFOP), Morro do Cruzeiro, Bauxita, Ouro Preto, 35400-000, Minas Gerais, Brazil

^c Centro Federal de Educação Tecnológica (CEFET), Av. Amazonas, 5253, Belo Horizonte, 30421-169, Minas Gerais, Brazil

ARTICLE INFO

Article history:

Received 16 May 2016

Received in revised form 14 June 2016

Accepted 15 June 2016

Available online xxx

Keywords:

Glycerol

Sodium hydroxide

Alkoxide

Hydrogen

Syngas

ABSTRACT

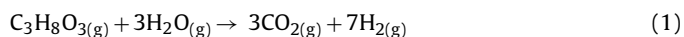
In this paper, it is proposed a new route, named “Alcoxycle”, for the conversion of glycerol from biodiesel production into H₂ and CO/CO₂ in different and separate stages. In this process, glycerol first reacts with NaOH to form an alkoxide that, in a second step, undergoes controlled thermal decomposition. Analyses of glycerol:NaOH precursor mixtures (molar ratios of 1:1, 1:2, 1:3 and 1:5) by TG, XRD, SEM, TEM, Raman, total carbon and GC–MS showed that the decomposition of the alkoxide at 400 °C leads to the formation of three fractions: liquid, gas and solid. The liquid products were formed only in very small amounts whereas an important gas fraction (12–16 wt%) was produced consisting mainly of H₂ (95% selectivity). In the second stage, the solid products (70–86 wt%) consisting of Na₂O, carbon and mostly Na₂CO₃ can be decompose by heating at 700 °C to produce CO₂ and especially CO. At the end of the Alcoxycle process, the NaOH used in the reaction and also the NaOH present in the biodiesel glycerol can be recovered and reused.

© 2016 Published by Elsevier B.V.

1. Introduction

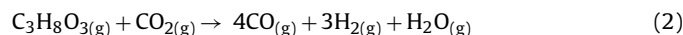
New strategies have been intensively investigated to develop processes to use the different biodiesel by-products. One of the main by-product is glycerol formed during the transesterification reaction, which contains 10–15% impurities based on water, oil, carboxylic acid/soaps and 5–10% of catalyst waste, typically NaOH [1].

Different routes to convert glycerol into several products have been studied in the last years [2–6], e.g. 1,3-propanediol and dihydroxyacetone, organic acids from biological route [7], acrolein [8–10], fuel additives [11], polymers [12] and oligomers with different applications such as dust suppressor [13]. The conversion of glycerol into syngas, H₂ and CO, has been receiving considerable attention lately [14,15]. Different reform strategies have been investigated such as steam, liquid phase, supercritical, dry and autothermal. The steam reform consists in the reaction of glycerol with water (Eq. (1)) [16,17].

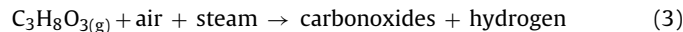


This reaction is endothermic and usually temperatures higher than 500 °C are used and side reactions such as water-gas shift and methanation commonly occur. This process produces H₂:CO ratio generally higher than 10, which is far from 2, the ideal syngas ratio for Fischer-Tropsch [18,19]. An alternative route is the aqueous phase reform which demands moderate temperatures (200–300 °C) but high pressures, e.g. 28–55 atm [20] affording relatively low yields. The reform in supercritical water consists in the same chemical processes (Eq. (1)) but the temperature and pressure must be higher than the critical point (T > 374 °C and P > 218 atm) [21]. Also, in general, these reform processes produce considerable amounts of undesirable chemical intermediates, e.g. acrolein [21].

The dry reform is done in the absence of water, using CO₂ as an oxidant (Eq. (2)) [19].



The autothermal reform is the combination of two processes, the steam reform and partial oxidation (Eq. (3)). This process offers an energetic advantage once the exothermic partial oxidation out-balances the endothermic steam reform [22,23].



* Corresponding author.

E-mail address: rochel@ufmg.br (R.M. Lago).

For most of these reform processes an important drawback is the need of a relatively expensive metal based catalyst which easily deactivates under the reaction conditions [14,24].

In this work, a new route to transform glycerol into H₂ and CO is proposed with significant advantages such as (i) the H₂ is produced in a different step from CO production, being possible to obtain these gases separately by a control of the temperature and (ii) the NaOH used as catalyst in the transesterification reaction (present as a contamination in the glycerol) can be recovered.

2. Materials and methods

All chemicals were used without previous treatment. The precursor were prepared reacting glycerol (Synth, 99,5%) with NaOH (Vetec, 99%) in molar ratios of 1:1, 1:2, 1:3 and 1:5 glycerol:NaOH (Glyc:1Na, Glyc:2Na, Glyc:3Na and Glyc:5Na, respectively). The resultant mixture was treated at 60 °C for 24 h and used directly in the further experiments. For the thermal decomposition, 80–120 mg of the precursors were placed in a tubular quartz reactor under a static argon atmosphere and heated (10 °C min⁻¹) in a ceramic furnace until 400, 550 and 900 °C for 1 h each. Three fractions were obtained: solid, liquid and gaseous.

The composition of the solid fraction was determined using several techniques. The X-ray diffraction (XRD) was performed in a Shimadzu equipment model XRD-7000, with Cu K α radiation, using the powder method. The Raman spectra was obtained in a Bruker equipment, model Senterra equipped with a CCD detector. Also, it is coupled with an optical microscopy (OLYMPUS BX51) to focus the laser beam and to collect the backscattered light. The spectra was done using the 633 nm laser with 2 mW of potency, integration time of 10 s and 10 co-additions. The SEM images were acquired in a Quanta 200 FEG equipment. The TEM images were obtained in a Tecnai G2-20 SuperTwin FEI 200 kV. Thermogravimetric analysis (TG) was done in a Shimadzu model DTG-60H with a nitrogen or air flux of 50 mL min⁻¹ up to 900 °C and heating rate of 10 °C min⁻¹. The total carbon (TC) in solution was performed in a Shimadzu equipment model TOC-V-CPH. For this analysis, deionized water was added to the crude solid and the mixture was then filtered to obtain a solution.

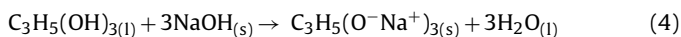
The liquid condensed at the trap were collected dissolving it at acetone (Quimex, 99,5%). Then, the products were characterized using gas chromatography in an Agilent® model GC-7890 coupled with a mass spectrometer Agilent® model 5975C with a quadrupole analyzer. The products were separated on a HP-5 column.

The gas produced were sampled and analyzed with gas chromatography in a Shimadzu model GC-2010. The permanent gases were separated on a Carboxen®-1010 column and analyzed in a thermal conductor detector (TCD).

The hydrocarbons gases were separated in the same column and analyzed with a flame ionization detector (FID). The CG was calibrated with a standard gas mixture containing H₂, CO, CO₂, CH₄, C₂H₆, C₂H₄ e C₂H₂ in N₂. The gas products were obtained in molar and indicated the variation of gas composition with respect to the precursor thermally decomposed.

3. Results and discussion

The alkoxide intermediates were prepared by the simple reaction of glycerol with sodium hydroxide with different NaOH/glycerol molar ratios, i.e. 1, 2, 3 and 5 (Eq. (4)).



The formation of these alkoxides has been described before [25]. These precursors are very hygroscopic and, after drying at 60 °C for 24 h, they were used directly for the experiments.

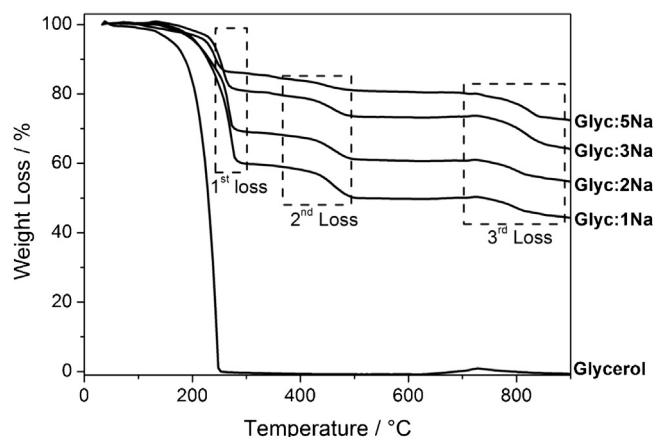


Fig. 1. TG analyses, in argon atmosphere, of the precursors Glyc:Na and glycerol.

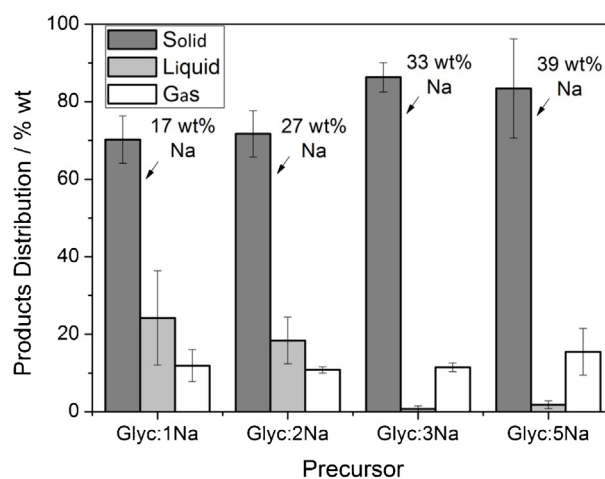


Fig. 2. Mass balance of the solid, liquid and gas fractions obtained for the decomposition of the different precursors at 400 °C.

Thermogravimetric analyses of the precursors (Fig. 1) showed three main weight losses at 150–300, 400–550 and 700–900 °C.

The first weight loss, up to 300 °C, is probably related to the loss of water, partial decomposition of the precursors and evaporation of excess glycerol. In fact, pure glycerol shows a 100% weight loss between 140 and 240 °C due to its evaporation (Fig. 1). The second weight loss, related to precursor decomposition, varies from 3 up to 10%. Above 700 °C, the weight loss is likely due to the decomposition of more stable compounds, most likely inorganics. In general, as the Na content in the precursor increased, all the losses decreased whereas the remained solid fraction present in the samples at 900 °C increased. Based on these results, the thermal decomposition of the substrates was investigated at 400, 550 and 900 °C.

Decomposition of the different precursors carried out at 400 °C produced three fractions: solid, liquid and gas. The obtained mass balances for these fractions are shown in Fig. 2.

For all precursors, the solid product represented ca. 70–90%. In this fraction 17–39% is related to the presence of Na⁺, likely in the form of oxides and carbonate salts. The liquid fraction was only significant for Glyc:1Na and Glyc:2Na. It can be observed that the gas fraction slightly increased from 12 to 18% as the Na content increased in the precursor.

The obtained grey solids showed a fraction soluble in HCl (1 M) leaving an insoluble black solid, suggesting the presence of carbon in these materials. SEM images of the raw grey solid (before acid

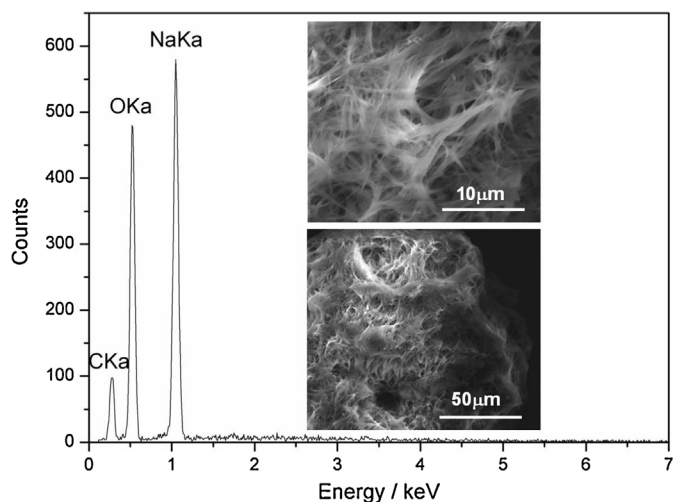


Fig. 3. SEM images and EDS for raw solid obtained by decomposition of the precursors at 400 °C.

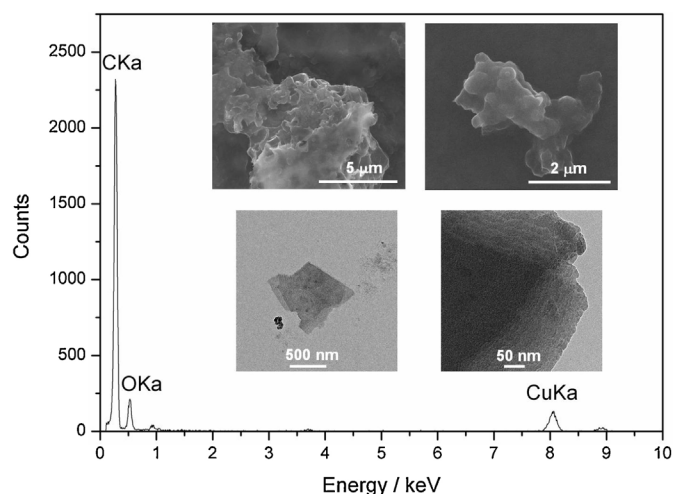


Fig. 4. SEM and TEM images and EDS for the washed solid obtained by decomposition of the precursors at 400 °C.

treatment) showed fibrous-needle-shaped structures, common for carbonate salts [26,27]. In fact, EDS analysis confirmed the presence of sodium, carbon and oxygen atoms (Fig. 3).

After acid wash, a completely different morphology was observed by SEM and the EDS spectrum suggests that the sodium was removed and only carbon was present. TEM images of the obtained black solid after washing suggested for most particles a graphite-like structure and in some cases few layers graphene structure (Fig. 4).

The Raman spectra for the raw solid presented a band near 1188 cm^{-1} , related to a carbonate (CO_3^-) $\nu_{\text{C-O}}$ stretching [28], and two bands due to the presence of carbon, i.e. D band related to less organized carbon structures and G band related to organized graphene structure [29] (Fig. 5). After washing with HCl these D and G band became more pronounced (see detail of Fig. 5)

The diffractogram for the raw solid samples were in perfect correlation with the pattern of Na_2CO_3 , according to JCDPS 37-457 (see Supplementary Material).

TG analyses of the raw solid obtained at 400 °C in air atmosphere showed an exothermic weight loss between 300 and 500 °C (see DTA in Supplementary Material) likely related to oxidation of the carbonaceous products (Fig. 6). The relatively low oxidation temperatures suggest the presence of a more amorphous reactive

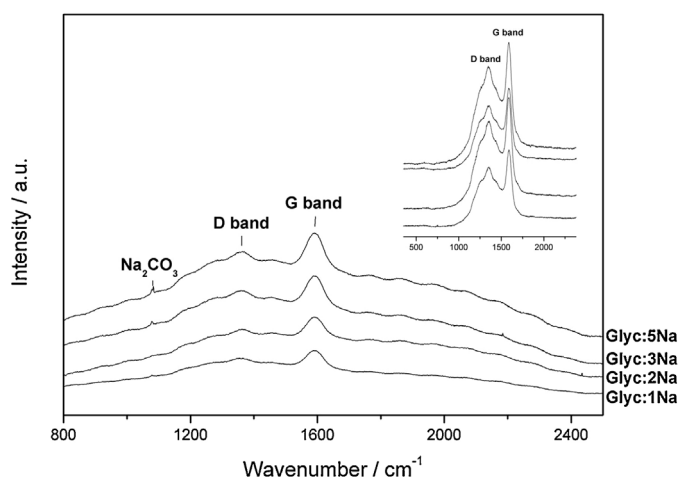


Fig. 5. Raman spectrum for the crude solid and for the washed solid (detail) obtained by decomposition of the precursors at 400 °C.

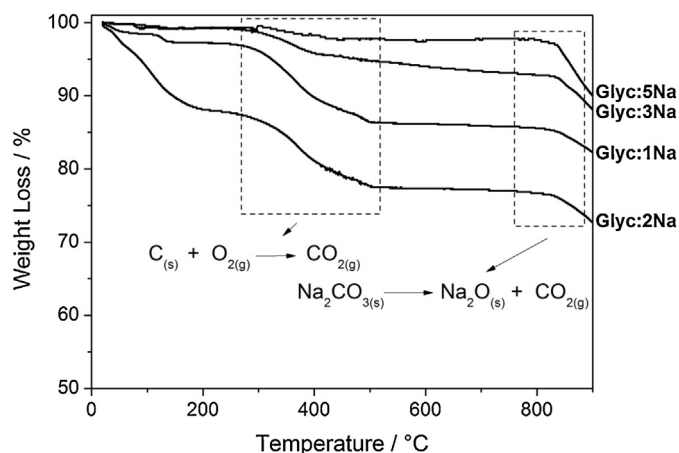


Fig. 6. TG analyses for the raw solid obtained by decomposition of the precursors at 400 °C.

Table 1

Composition of the solid fraction obtained by the decomposition of the different precursors at 400 °C.

Substrates	%C ^a	% Na_2CO_3 ^b	% Na_2O ^c
Glyc:1Na	11	85	4
Glyc:2Na	10	89	1
Glyc:3Na	4	85	11
Glyc:5Na	2	80	18

^a Determined by TG.

^b Determined by TC.

^c Calculated by difference.

carbon [30]. It can also be observed a weight loss near 850 °C likely related to the sodium carbonate decomposition.

The raw solid was solubilized in water and then filtered. The amount of carbonate was estimated from the remaining solution by TC (Total Carbon analysis). Thus, the composition of the solid fraction was determined using the amount of carbon estimated from TG, carbonate estimated from TC measurements and Na_2O from the difference (Table 1).

As it can be observed, carbonate salt represents the main component of the solid fraction, more than 80%. Also, as expected, the amount of Na_2O increases for the precursors with higher Na content, while the opposite occurs for carbon.

Only very small amounts of liquid products were formed during the thermal decomposition for the substrates Glyc:1Na and

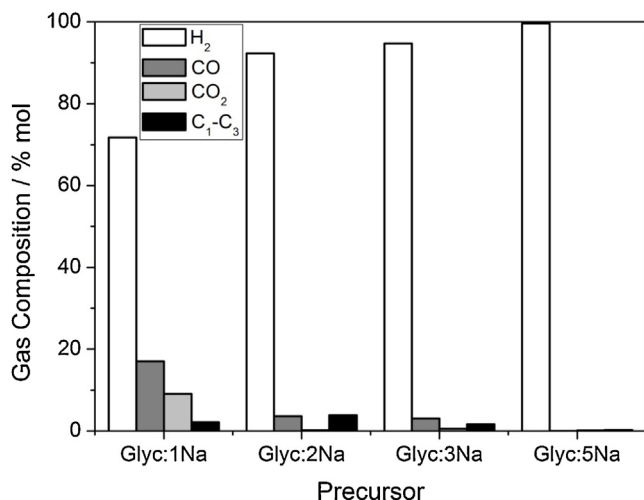


Fig. 7. Gas composition obtained for the different precursors decomposed at 400 °C.

Glyc:2Na at 400 °C, i.e. ca. 20%. In these samples, GC–MS analysis showed that non-reacted glycerol was the main component and traces of 1,2-propanediol were identified. The other substrates Glyc:3Na and Glyc:5Na showed only traces of liquid derivatives. The gas products formed up to 400 °C, collected and identified by GC, were composed mainly by H₂, very small amounts of CO, CO₂, CH₄ and traces of hydrocarbons C₂ and C₃. As shown in Fig. 7, the selectivity for H₂ increased for the substrates with excess of NaOH in its preparation, reaching 99% for Glyc:5Na. Onwudili and Williams [31] studied the role of NaOH in hydrothermal reactions with several biomass samples such as cellulose, glucose, starch and others. It was observed that the presence of NaOH favoured the gasification reactions and the production of H₂. Some mechanistic studies [32,33] suggested that the NaOH reacts with CO₂ to form Na₂CO₃ or NaHCO₃ favouring the Water Gas Shift reaction.

For the Alkoxyde investigated in this work, only in the first decomposition step, the calculated H₂ production was 4.7 mol of a theoretical maximum of 5.5 mol which corresponds to a 85% yield for Glyc:3Na, considering all hydrogen atoms from glycerol and NaOH.

The second stage of thermal decomposition (observed in the TG curves near 500 °C) was also investigated by collecting the gases only in the second decomposition, between 400 and 550 °C. GC analyses showed the presence of mainly CO and small amounts of CO₂ and H₂ (Fig. 8). The precursor Gly:5Na did not produce significant amount of gas in the temperature range 400–550 °C as observed by TG in Fig. 1.

The gases formed in the third stage of the thermal decomposition (observed in the TG curves after 700 °C) was also investigated. The gases were collected between 550 and 900 °C and analyzed by GC. It can be observed that the main gases are CO and CO₂, especially for the Glyc:2Na, Glyc:3Na and Glyc:5Na precursors (Fig. 9).

The high amount of CO and CO₂ at this temperature is likely related to two reactions, the Na₂CO₃ decomposition (Eq. (5)) and also the reverse Boudouard reaction (Eq. (6)) which should be favoured at 900 °C [34,35].



After thermal decomposition (900 °C), the remaining white solid was completely soluble in water and strongly alkaline. Moreover, TC analysis of the solution also showed the absence of carbonates, suggesting the presence of only Na₂O. Based on the results obtained in this work some considerations can be made on the Alkoxyde.

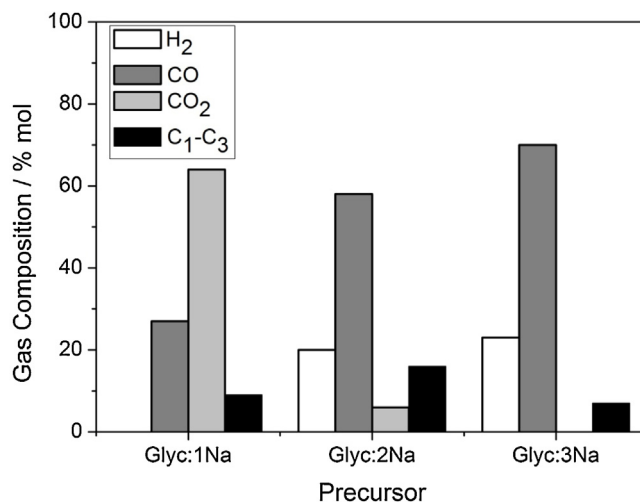


Fig. 8. Gas composition in the range of 400–550 °C.

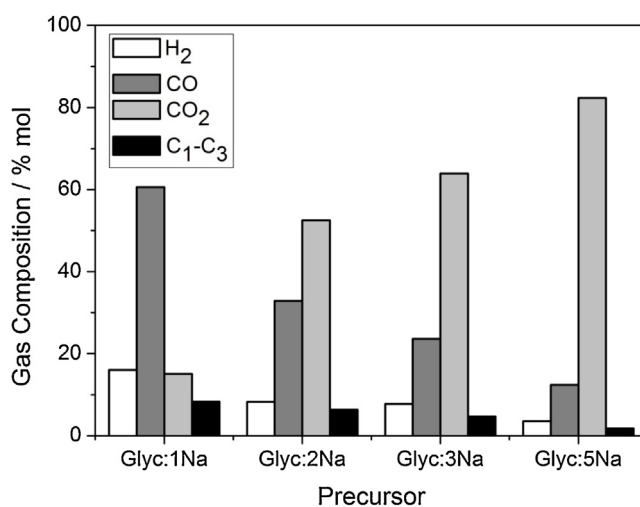
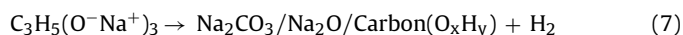


Fig. 9. Gas composition in the range of 550–900 °C.

When low Na contents are used, i.e. Glyc: 1Na and Glyc:2Na, a liquid product is formed. This fraction is a result of glycerol evaporation combined with other process, e.g. alkoxyde decomposition to form glycerol derivatives and other reactions promoted by the strong alkaline medium. This liquid is, therefore, a complex mixture of different compounds with no direct application. When molar ratios NaOH:glycerol higher than 3:1 are used, no significant amount of liquid product is formed. These results suggest that the combination of 1Na atom for 1O atom of glycerol induces the complete collapse of the glycerol to form only small gas molecules. Apparently, in the first thermal decomposition step most of the oxygen and carbon atoms will remain in the solid phase as carbonate. Some of the C atoms aromatize to form a solid carbon containing relatively high concentration of oxygen functionalities and produce H₂ (Eq. (7)).



Although the process taking place in the second decomposition stage is not clear, one possibility is the decomposition of the high functionalized carbon to lose small amounts of H₂ and oxygen as CO and CO₂ (Eq. (8)).



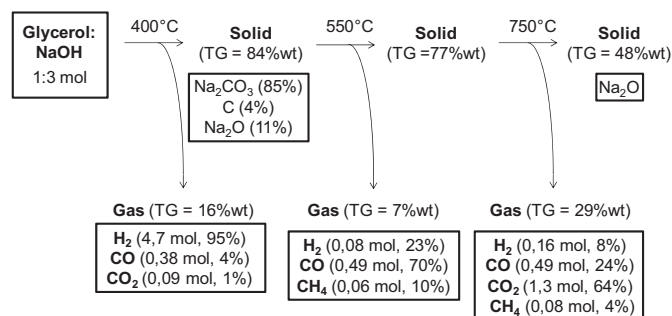


Fig. 10. Summary of complete thermal decomposition of the precursor Glyc:3Na.

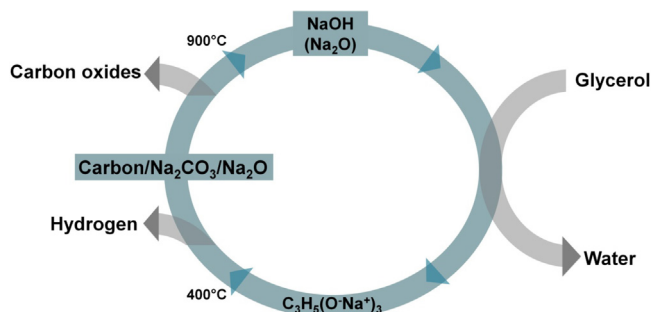


Fig. 11. Representation of the "Alcoxycle" for the production of H₂ and CO/CO₂ from glycerol and NaOH.

In the third stage at temperatures higher than 700 °C, apparently the sodium carbonate decomposes to produce CO₂ and, by a reaction with the carbon, produces CO.

Fig. 10 represents a summary of all thermal decomposition steps for the precursor Glyc:3Na. At 400 °C, H₂ was produced with high selectivity (95%) and yield of 4.7 of a nominal maximum of 5.5 mol (85%), considering all hydrogen atoms from glycerol and sodium hydroxide. The yield was calculated using the results from thermogravimetric analysis and gas chromatography. In the second and third decomposition stages, CO and CO₂ were the main products, 70 and 64%, respectively. These results suggest that is possible to produce H₂ with high selectivity in a different step, separated from the other gases, mainly CO_x.

Fig. 11 represents the complete Alcoxycle, where basically hydrogen is produced at 400 °C and a mixture of CO/CO₂ was obtained at 900 °C. Furthermore, only Na₂O was observed at the end of the process, showing a possibility of recovering the NaOH.

An important aspect of this process is the energy consumption. Detailed study on the thermodynamics and energy balance is currently in progress. However, one can envisage that compared to the other glycerol conversion processes, i.e. steam, dry and autothermal reform, the energy consumption should be similar.

4. Conclusion

Thermal decomposition of Na⁺ alkoxides from glycerol at 400 °C produces mainly H₂ with selectivity of 95 mol% and 85% yield for Glyc:3Na. The solid fraction is composed mainly by Na₂CO₃, but also contained Na₂O and carbon. Further treatment up to 900 °C produced mainly CO and CO₂. This cyclic process showed very promising results to convert glycerol to syngas with the advantages of producing H₂ and CO_x in separate and different stages as well as recovering the NaOH present in the glycerol from the biodiesel process.

Acknowledgments

The authors are grateful for the financial support for this work by Petrobras, FAPEMIG, CAPES and CNPq. The authors would like to acknowledge the Center of Microscopy at the Universidade Federal de Minas Gerais (<http://www.microscopia.ufmg.br>) for providing the equipment and technical support for experiments involving electron microscopy.

Appendix A. Supplementary data

Supplementary data associated with this article can be found, in the online version, at <http://dx.doi.org/10.1016/j.cattod.2016.06.039>.

References

- [1] M. Zhang, H. Wu, Effect of major impurities in crude glycerol on solubility and properties of glycerol/methanol/bio-oil blends, *Fuel* 159 (2015) 118–127.
- [2] M. Ayoub, A.Z. Abdullah, Critical review on the current scenario and significance of crude glycerol resulting from biodiesel industry towards more sustainable renewable energy industry, *Renew. Sustain. Energy Rev.* 16 (2012) 2671–2686.
- [3] A.B. Leoneti, V. Aragão-Leoneti, S.V.W.B. de Oliveira, Glycerol as a by-product of biodiesel production in Brazil: alternatives for the use of unrefined glycerol, *Renew. Energy* 45 (2012) 138–145.
- [4] C.J.A. Mota, *Gliceroquímica: novos produtos e processos a partir da glicerina de produção de biodiesel*, Sociedade Brasileira de Química, 2009.
- [5] C.A.G. Quispe, C.J.R. Coronado, J.A. Carvalho Jr., Glycerol Production, consumption, prices, characterization and new trends in combustion, *Renew. Sustain. Energy Rev.* 27 (2013) 475–493.
- [6] H.W. Tan, A.R. Abdul Aziz, M.K. Aroua, Glycerol production and its applications as a raw material: a review, *Renew. Sustain. Energy Rev.* 27 (2013) 118–127.
- [7] G.P. da Silva, M. Mack, J. Contiero, Glycerol: a promising and abundant carbon source for industrial microbiology, *Biotechnol. Adv.* 27 (2009) 30–39.
- [8] A. Corma, G.W. Huber, L. Sauvanaud, P. O'Connor, Biomass to chemicals: catalytic conversion of glycerol/water mixtures into acrolein reaction network, *J. Catal.* 257 (2008) 163–171.
- [9] B. Katryniok, S. Paul, V. Belliere-Baca, P. Rey, F. Dumeignil, Glycerol dehydration to acrolein in the context of new uses of glycerol, *Green Chem.* 12 (2010) 2079–2098.
- [10] L. Ott, M. Bicker, H. Vogel, Catalytic dehydration of glycerol in sub- and supercritical water: a new chemical process for acrolein production, *Green Chem.* 8 (2006) 214–220.
- [11] N. Rahmat, A.Z. Abdullah, A.R. Mohamed, Recent progress on innovative and potential technologies for glycerol transformation into fuel additives: a critical review, *Renew. Sustain. Energy Rev.* 14 (2010) 987–1000.
- [12] M. de Araújo Medeiros, M.T.C. Sansiviero, M.H. Araújo, R.M. Lago, Modification of vermiculite by polymerization and carbonization of glycerol to produce highly efficient materials for oil removal, *Appl. Clay Sci.* 45 (2009) 213–219.
- [13] M.A. Medeiros, C.M.M. Leite, R.M. Lago, Use of glycerol by-product of biodiesel to produce an efficient dust suppressant, *Chem. Eng. J.* 180 (2012) 364–369.
- [14] S. Adhikari, S.D. Fernando, A. Haryanto, Hydrogen production from glycerol: an update, *Energy Convers. Manage.* 50 (2009) 2600–2604.
- [15] P.D. Vaidya, A.E. Rodrigues, Glycerol reforming for hydrogen production: a review, *Chem. Eng. Technol.* 32 (2009) 1463–1469.
- [16] S. Adhikari, S. Fernando, A. Haryanto, Production of hydrogen by steam reforming of glycerol over alumina-supported metal catalysts, *Catal. Today* 129 (2007) 355–364.
- [17] T. Hirai, N.-o. Ikenaga, T. Miyake, T. Suzuki, Production of hydrogen by steam reforming of glycerol on ruthenium catalyst, *Energy Fuels* 19 (2005) 1761–1762.
- [18] E.L. Kunkes, R.R. Soares, D.A. Simonetti, J.A. Dumesic, An integrated catalytic approach for the production of hydrogen by glycerol reforming coupled with water-gas shift, *Appl. Catal. B: Environ.* 90 (2009) 693–698.
- [19] H.C. Lee, K.W. Siew, J. Gimbin, C.K. Cheng, Synthesis and characterisation of cement clinker-supported nickel catalyst for glycerol dry reforming, *Chem. Eng. J.* 255 (2014) 245–256.
- [20] R.D. Cortright, R.R. Davda, J.A. Dumesic, Hydrogen from catalytic reforming of biomass-derived hydrocarbons in liquid water, *Nature* 418 (2002) 964–967.
- [21] E. Markočič, B. Kramberger, J.G. van Bennekom, H. Jan Heeres, J. Vos, Ž. Knez, Glycerol reforming in supercritical water: a short review, *Renew. Sustain. Energy Rev.* 23 (2013) 40–48.
- [22] G. Nahar, V. Dupont, Recent advances in hydrogen production via autothermal reforming process (ATR): a review of patents and research articles, *Recent Pat. Chem. Eng.* 6 (2013) 8–42.
- [23] D.C. Rennard, J.S. Kruger, B.C. Michael, L.D. Schmidt, Long-time behavior of the catalytic partial oxidation of glycerol in an autothermal reactor, *Ind. Eng. Chem. Res.* 49 (2010) 8424–8432.

- [24] M. El Doukkali, A. Iriondo, J.F. Cambra, P.L. Arias, Recent improvement on H₂ production by liquid phase reforming of glycerol: catalytic properties and performance, and deactivation studies, *Top. Catal.* 57 (2014) 1066–1077.
- [25] H.S. Fry, E.L. Schulze, The liberation of hydrogen from carbon compounds. IV. the interaction of glycol and glycerol with fused caustic alkalies, *J. Am. Chem. Soc.* 50 (1928) 1131–1138.
- [26] J. Jiang, M.-R. Gao, Y.-H. Qiu, G.-S. Wang, L. Liu, G.-B. Cai, S.-H. Yu, Confined crystallization of polycrystalline high-magnesium calcite from compact Mg-ACC precursor tablets and its biological implications, *CrystEngComm* 13 (2011) 952–956.
- [27] M. Wang, H.K. Zou, L. Shao, J.F. Chen, Controlling factors and mechanism of preparing needlelike CaCO₃ under high-gravity environment, *Powder Technol.* 142 (2004) 166–174.
- [28] S. Gunasekaran, G. Anbalagan, S. Pandi, Raman and infrared spectra of carbonates of calcite structure, *J. Raman Spectrosc.* 37 (2006) 892–899.
- [29] A.C. Ferrari, J. Robertson, Interpretation of Raman spectra of disordered and amorphous carbon, *Phys. Rev. B* 61 (2000) 14095–14107.
- [30] J.P. Trigueiro, G.G. Silva, R.L. Lavall, C.A. Furtado, S. Oliveira, A.S. Ferlauto, R.G. Lacerda, L.O. Ladeira, J.W. Liu, R.L. Frost, G.A. George, Purity evaluation of carbon nanotube materials by thermogravimetric, TEM, and SEM methods, *J. Nanosci. Nanotechnol.* 7 (2007) 3477–3486.
- [31] J.A. Onwudili, P.T. Williams, Role of sodium hydroxide in the production of hydrogen gas from the hydrothermal gasification of biomass, *Int. J. Hydrogen Energy* 34 (2009) 5645–5656.
- [32] J.A. Onwudili, P.T. Williams, Reaction of different carbonaceous materials in alkaline hydrothermal media for hydrogen gas production, *Green Chem.* 13 (2011) 2837–2843.
- [33] J.A. Onwudili, P.T. Williams, Hydrothermal reactions of sodium formate and sodium acetate as model intermediate products of the sodium hydroxide-promoted hydrothermal gasification of biomass, *Green Chem.* 12 (2010) 2214–2224.
- [34] Y. Jiao, W. Tian, H. Chen, H. Shi, B. Yang, C. Li, Z. Shao, Z. Zhu, S.-D. Li, In situ catalyzed Boudouard reaction of coal char for solid oxide-based carbon fuel cells with improved performance, *Appl. Energy* 141 (2015) 200–208.
- [35] P. Lahijani, Z.A. Zainal, M. Mohammadi, A.R. Mohamed, Conversion of the greenhouse gas CO₂ to the fuel gas CO via the Boudouard reaction: a review, *Renew. Sustain. Energy Rev.* 41 (2015) 615–632.